Synthesis of Abnormal Immunoglobulins by Hybridomas from Autoimmune "Viable Motheaten" Mutant Mice

Peter A. Schweitzer, Suzanne E. Taylor, and Leonard D. Shultz

The Jackson Laboratory, Bar Harbor, Maine 04609

Abstract. Secretory defects in abnormal plasma cells, called Mott cells, that appear in lymphoid tissues of spontaneously autoimmune, "viable motheaten" (*me^v/me^v*) mice lead to deposition of immunoglobulin in RER-bound vesicles. Such vesicles have been termed Russell bodies. Cells with Russell bodies can also be observed rarely in normal animals, usually as a result of extreme antigenic loads or pathologic states. To understand why these abnormal cells appear commonly in *me^v/me^v* mice, we have established a panel of hybridomas that contain Russell bodies. Using immunochemical analysis and immunoelectron microscopy, we have characterized the secretory defects. Although these hybridoma cells synthesize a normal size heavy chain and it associates with light chain, the Russell bodies have many characteristics of inclusion bodies, which commonly appear in cells synthesizing mutant proteins and often are associated with incompletely or abnormally folded proteins. Pulse-chase experiments showed that immunoglobulins synthesized by these hybridomas accumulate rapidly into insoluble complexes and have an intracellular half life ~10 time greater than normal immunoglobulins. The defect affected only the immunoglobulin derived from the *me^v/me^v* mice and did not affect the secretion of normal immunoglobulin produced by an IgG1-secreting fusion partner. In addition to accumulating intracellular immunoglobulins, many mutant cell lines also secreted immunoglobulin. Endoglycosidase H digestion was used to determine the state of processing of the *N*-linked carbohydrates on the immunoglobulin molecules. This analysis demonstrated that the *N*-linked carbohydrates on the secreted immunoglobulin were resistant to endoglycosidase H digestion, indicating that they were processed normally. The insoluble IgM molecules were sensitive to endoglycosidase H, which is consistent with their localization to the RER. We propose several models by which these abnormal immunoglobulin-secreting cells commonly appear in this autoimmune mutant mouse.

MUTATIONS that disrupt biological processes provide insight into the ordering of these processes. Many mutations that affect the immune system cause multiple pleiotropic abnormalities, emphasizing the complexity and interrelatedness of the immune, endocrine, and nervous systems (33). One of the most deleterious mutations identified is "viable motheaten" (*me^v*),[1] a spontaneous, single gene mutation that occurred on the C57BL/6J background (34). *me^v* mice have a mean life span of 9 wk. Autoimmune pulmonary lesions are the proximal cause of death. Homozygotes (*me^v/me^v*) develop glomerulonephritis, have multiple autoantibodies, and serum IgM levels are increased 25- to 50-fold above levels found in littermate controls (35). Abnormal plasma cells, called Mott cells, are found initially at ~4 wk of age. These cells have discrete glycoprotein inclusions, termed Russell bodies. Such inclusions are RER-bound vesicles containing Ig.

Although Mott cells have been recognized since 1890 (29), neither the factors responsible for their development nor the role of these cells in normal and in disease states is understood. While Mott cells are rare in normal tissues (22), they appear in patients with multiple myeloma (24), trypanosomiasis (28), and AIDS (4). White (38) determined that Mott cells could be induced in rabbits and mice by hyperimmunization with crude bacterial preparations and the Ig present in Mott cells was often antigen specific. Mott cells are phenotypically heterogeneous, in vivo, and can be found with globular, "medusoid," or crystalline Russell bodies. Also, T cells play an unidentified role in the development of Mott cells (35). Although several Mott cell hybridomas have been analyzed biochemically (1, 2, 36), the underlying cause of Russell body formation has remained unknown.

In this report, we describe the generation of permanent, somatic cell hybrids that retain characteristics of Mott cells. Biochemical characterization and immunoelectron microscopy were used to study the nature of the secretory defects.

1. *Abbreviations used in this paper*: BiP, binding protein; Endo H, endoglycosidase H; *me^v*, viable motheaten; PAS, periodic acid-Schiff's; SACI, *Staphylococcus aureus*, Cowan strain I; TEM, transmission electron microscopy.

The secretory defect affected only the *me^v/me^v*-derived Ig and in the majority of hybridomas the solubility of the Ig was affected. The Russell bodies described here have many characteristics of inclusion bodies, which are commonly found associated with the production of mutant proteins or when eukaryotic proteins are expressed in bacteria by recombinant DNA techniques. Deposition of proteins in inclusion bodies is thought to occur when proteins are incompletely or abnormally assembled or folded improperly.

Materials and Methods

Mice and Cell Lines

C57BL/6J-*me^v*/+ mice were bred in our research colony at The Jackson Laboratory. Homozygous *me^v/me^v* mice were identified by their characteristic skin lesions. The SP2/0 cell line (31) was obtained from Dr. I. Egorov (The Jackson Laboratory) and the P3X63Ag8 cell line (17) was obtained from the ATCC cell line repository. Both cell lines were grown in HY medium (Sigma Chemical Co., St. Louis) supplemented with hypoxanthine, thymidine, and 10% FCS. The tissue culture medium also contained 0.13 mM 8-azaguanine to ensure their sensitivity to aminopterin.

Hybridomas and Screening Protocols

Single-cell suspensions were made by pressing cervical lymph nodes though Nitex nylon mesh (TETKO Inc., Elmsford, NY) into RPMI 1640 medium supplemented with 10% FCS and 25 mM Hepes buffer. Cells were washed by centrifugation, and viable cells were enumerated in a hemocytometer by trypan blue exclusion. Somatic cell hybridization was performed according to the procedure of Gefter et al. (9) using 30% polyethylene glycol 1,300–1,600 (Sigma Chemical Co.). Aminopterin-resistant hybridomas were screened within 3 wk of the fusion following deposition of $\sim 10^5$ cells on microscope slides with a cytocentrifuge. Cells were fixed in neutral-buffered formalin, stained with periodic acid-Schiff's (PAS) reagent (14) followed by hematoxylin, and examined microscopically for the presence of Russell bodies. Immunofluorescence microscopy was performed on cytocentrifuge slides fixed for 15 s in acetone. Directly fluoresceinated anti-mouse Ig isotype antibodies were obtained from Southern Biotechnology Associates (Birmingham, AL). Slides were examined by epifluorescence microscopy.

Transmission EM

Cell pellets were fixed in 2% glutaraldehyde, 1% paraformaldehyde in 0.1 M cacodylate buffer, pH 7.4. The pellets were then postfixed in 1% osmium tetroxide, stained en bloc with 0.5% uranyl acetate, dehydrated in ethanol, and embedded in Epon-araldite. Ultrathin sections were stained again with uranyl acetate followed by lead citrate. The specimens were viewed in an electron microscope (model 100 CXII; JEOL USA, Peabody, MA).

Protein A-immunogold EM

Thin sections fixed as described above were collected on colloidon-coated nickel grids, which were then floated on drops of saturated sodium metaperiodate for 1 h, by a modification of the method of Roth et al. (28*a*). Grids were then rinsed in distilled water and placed on drops of 1% BSA in PBS for 30 min. The grids were then placed on a drop containing primary antiserum and incubated overnight at 4°C. The primary antiserum was either rabbit anti-mouse μ chain (Southern Biotechnology Associates), rabbit anti-mouse γ1 chain (Zymed Labs, Inc., San Francisco, CA), or normal rabbit serum as a negative control. After incubation with antiserum or normal rabbit serum, the grids were washed in water, floated on drops of 1% BSA in PBS for 30 min, and then placed on drops of the protein A-gold-15 solution (Janssen Pharmaceutica, Beerse, Belgium) for 1 h. Finally, the grids were washed in distilled water and counterstained in uranyl acetate and lead citrate, and viewed as described above.

Metabolic Labeling and Lysates

10^5 hybridoma cells were labeled in vitro at 37°C in 0.25 ml methionine-free RPMI 1640 supplemented with 50 μCi/ml ^{35}S-methionine (New England Nuclear, Boston, MA; >800 Ci/mmol). Methionine-free medium was "deficient RPMI 1640" (Sigma Chemical Co.) supplemented with 2 mM glutamine, 0.38 mM leucine, 0.22 mM lysine, and 10% FCS that had been dialyzed extensively against 0.85% NaCl. After 3 h, cells were centrifuged for 8 min at 125 *g*. The supernatants were collected and kept in ice. The cells were washed by centrifugation and NP-40 lysates were prepared by suspending cells in 1 ml 50 mM Tris-HCl, 150 mM NaCl, pH 8.2, with 0.5% NP-40 (Calbiochem-Behring Corp., San Diego, CA), 1 U/ml aprotinin (Calbiochem-Behring Corp.), and 2 mM PMSF (Calbiochem-Behring Corp.). Cells were homogenized with 24 strokes in a Dounce homogenizer (pestle A) and centrifuged for 20 min at 27,000 *g* at 4°C. Russell bodies were solubilized from the pellets from the NP-40 lysates in 0.1 ml of 50 mM Tris-HCl, pH 8.2, with 1% SDS, 1 U/ml aprotinin, and 2 mM PMSF, at room temperature. In some experiments, lysates were made with lithium dodecyl sulfate (Boehringer Mannheim Biochemicals, Indianapolis, IN), which was used at 4°C. Lysates were made with 24 strokes in a Dounce homogenizer, then 0.9 ml of 50 mM Tris-HCl, pH 8.2, 0.56% NP-40, and 0.56 sodium deoxycholate (Sigma Chemical Co.) was added, given 12 additional strokes, and centrifuged for 20 min at 27,000 *g* at 4°C. The supernatants and lysates were kept in ice for subsequent immunoprecipitations.

Immunoprecipitations

When only IgM was to be analyzed, supernatants and lysates were precleared with 50 μl of a 10% suspension of *Staphylococcus aureus*, Cowan strain I (SACI). SACI had been previously washed by centrifugation twice with 50 mM Tris-HCl, 150 mM NaCl, pH 8.2, 5 mM EDTA, and 0.5% NP-40. The final, 10% suspension contained 1 mg/ml BSA in the buffer used to wash the SACI. After preclearing 15 min, SACI was removed by centrifugation, and 65 μg rabbit anti-mouse μ (Southern Biotechnology Associates) was added to each sample. For the analysis of IgG1 synthesis, samples were not precleared with SACI, and lysates were treated with either 6 μl normal rabbit serum, 65 μg rabbit anti-mouse μ, or 10 μl of a polyspecific rabbit anti-mouse Ig antiserum. The latter was an ammonium sulfate cut of serum from a rabbit immunized with normal mouse Igs. After 30 min of incubation with the antibodies, 50 μl SACI was added to each tube and incubated an additional 15 min in ice. Immunoprecipitates were collected by centrifugation, washed three times with 50 mM Tris-HCl, pH 8.2, 150 mM NaCl, 5 mM EDTA, and 0.5% NP-40. Each sample was suspended in 50 μl SDS-PAGE sample buffer (19).

Pulse-chase Experiments

Hybridoma cells were starved for 1 h in methionine-free medium at 4×10^6 cells/ml and then pulsed with 100 μCi/ml ^{35}S-methionine for 15 min. After the cells were washed twice in RPMI 1640 plus 10% FCS, labeled proteins were chased at 2×10^5 cells/ml for the indicated periods of time in RPMI 1640 supplemented with 10% FCS, 2 mM glutamine, and 5×10^{-5} M 2-mercaptoethanol. Immunoglobulins in supernatants and lysates were immunoprecipitated as described above.

Endoglycosidase H Treatment

For endoglycosidase H (endo H) digestion, immunoprecipitates were suspended in 50 mM Pipes (Sigma Chemical Co.), pH 6.5, 100 mM NaCl, 0.1 mg/ml BSA, 0.1% NP-40, and 1 mM PMSF. Each sample was divided into equal parts and one was digested with 10 mU endo H (Boehringer Mannheim Biochemicals, Inc.) at 37°C, overnight. The control samples were treated identically, without glycosidase addition. An equal volume of 2× SDS-PAGE sample buffer (19) was added before electrophoresis.

SDS-PAGE and Fluorography

Immunoprecipitated proteins were dissociated from the SACI, denatured, and reduced by incubation in a boiling water bath for 3 min. The SACI was removed by centrifugation and each sample was subjected to electrophoresis on 10% discontinuous SDS-polyacrylamide gels (19). After electrophoresis, proteins were fixed in the gels with 25% isopropanol and 10% acetic acid and then impregnated with the fluor, Enhance (New England Nuclear). Gels were dried and subjected to fluorography using X-Omat AR film (Eastman Kodak Co., Rochester, NY). The film had been sensitized previously by preflashing to an OD of $\sim$0.2.

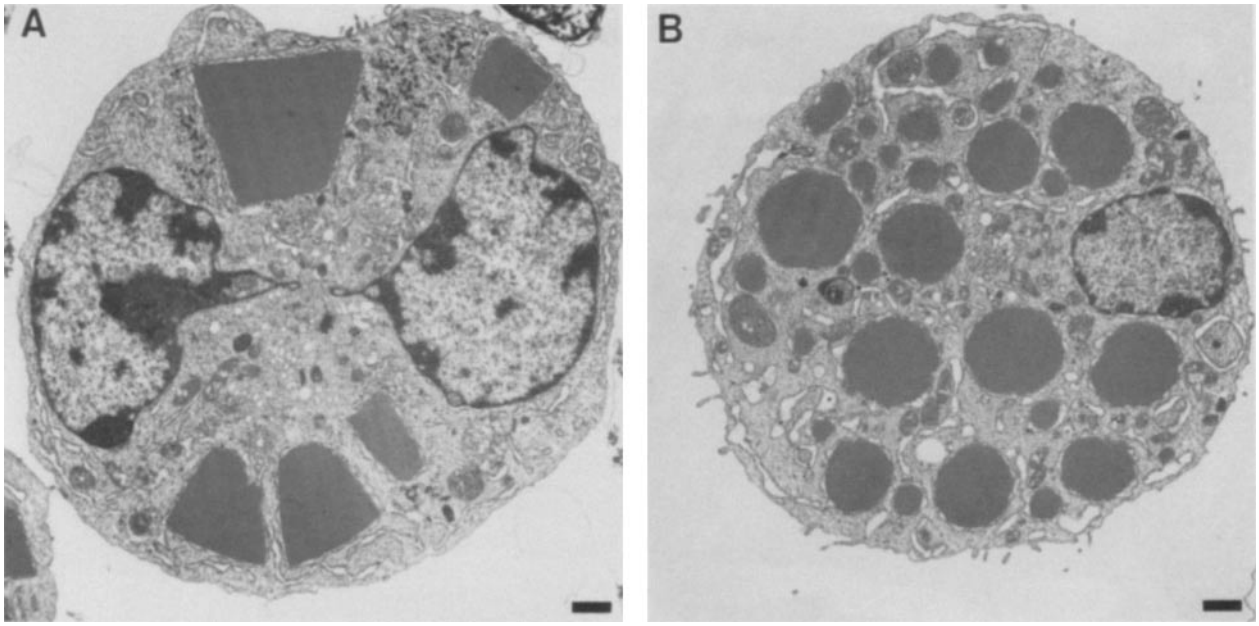

Figure 1. Transmission electron micrographs of Mott cell hybridomas. Two examples of Mott cell hybridomas grown in tissue culture, harvested, and prepared for transmission EM. (*A*) The D3 cell line that contained crystalloid Russell bodies. (*B*) The D8 cell line that contained spheroidal and "medusoid," Russell bodies. Bar, 1 μ.

Results

Construction and Identification of Mott Cell Hybridomas

Permanent cell lines (hybridomas) were constructed from cervical lymph node cells from me^v/me^v mice by polyethylene glycol–mediated somatic cell hybridization. Cervical lymph node cells are the richest source of Mott cells from these mutant mice (35). Spleen cells were not used because of the presence of an insidious population of rapidly proliferating macrophages. Hybridomas were screened for the presence of Russell bodies with PAS. From four independent fusions, and a total of 114 hybridomas screened, an average of 31% of the hybridomas had Russell bodies. We refer to these hybridomas with Russell bodies as Mott cell hybridomas although few achieve the classical "cluster of grapes" morphology. Because this was an unusual screening procedure, we examined 61 additional hybridomas generated from the spleens of hyperimmunized, +/+ mice and found that none had Russell bodies.

By transmission electron microscopy (TEM), several distinct and individual morphological types of Russell bodies were found in the Mott cell hybridomas (Fig. 1). Several of the morphological types described in vivo (35) were observed in the hybridomas. Globular, "medusoid," and crystalloid forms of Russell bodies have been found in the hybridomas. Although these morphologic types have been placed into a general progression from globular to medusoid to crystalline (35) each hybridoma was stable and no "progression" in vitro was noted. The crystalline Russell bodies shown in Fig. 1 *A* appeared irregular by TEM, but using phase contrast microscopy or PAS-stained, fixed specimens, these Russell bodies appeared to be regular tetrahedrons. The parent SP2/0 cell line had no Russell bodies.

Immunofluorescence staining of Mott cell hybridomas was used to determine the Ig isotype produced by each hybridoma. Cytocentrifuge slides were stained with directly fluoresceinated anti-isotype reagents and visualized by epifluorescence microscopy. All hybridomas made IgM, of which the majority had κ light chains, although λ light chains were detected in a minority of hybridomas (not shown).

Biochemical Analysis of IgM from Different Mott Cell Hybridomas

During our initial biochemical analysis of Ig synthesized by hybridomas with Russell bodies, we found that a large pool of intracellular Ig remained insoluble in 0.5% NP-40. Ordinarily, 0.5% NP-40 lysis buffers are sufficient to solubilize transmembrane proteins and intraluminal proteins from intracellular membranous compartments. The insoluble residue following 0.5% NP-40 treatment was examined by TEM, and although the RER membrane had been removed, Russell bodies remained intact (not shown). The Russell bodies could be solubilized by homogenizing the insoluble material from the NP-40 lysate in 1% SDS (heretofore referred to as the SDS lysate) or other denaturing conditions, such as 6 M guanidine HCl. In Fig. 2, IgM molecules immunoprecipitated from the supernatants, the NP-40 lysates, and the SDS lysates of several hybridomas from me^v/me^v mice are shown. In the first three lanes, IgM from the supernatant, NP-40 lysate, and SDS lysate from phenotypically normal (non-Mott cell) hybridoma is shown. The μ chain from the secreted IgM is slightly larger than the intracellular form because of carbohydrate processing (15). No IgM was precipitated from the SDS lysate (2E7, DS) from this hybridoma, which lacked Russell bodies. Although this "normal" hybridoma was also derived from me^v/me^v mice, the relative mobility of its μ chain is indistinguishable from μ chains from

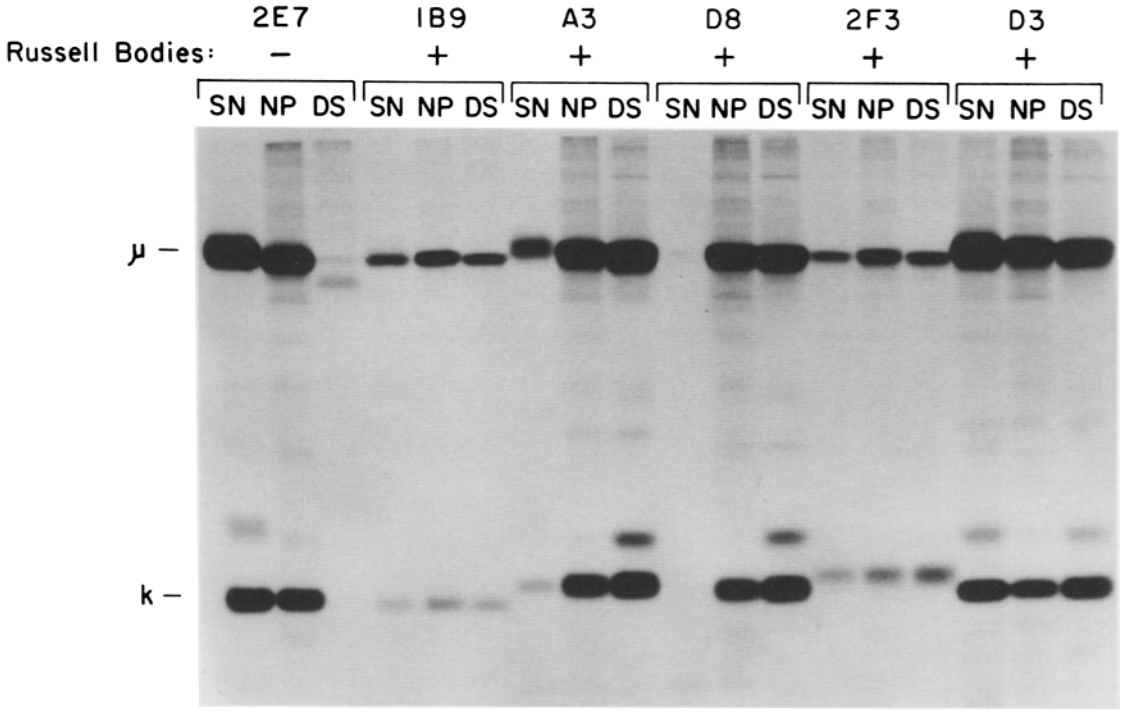

Figure 2. Immunoglobulins synthesized by different cell lines. Six different hybridomas from me^v/me^v mice were labeled with ^{35}S-methionine for 3 h. The supernatants (*SN*), NP-40 lysates (*NP*), and SDS lysates (*DS*) were treated with rabbit anti-μ and Igs were precipitated with protein A-bearing SACI organisms. Each precipitate was subjected to SDS-PAGE and fluorography. The 2E7 hybridoma had no Russell bodies. The 1B9, A3, D8, 2F3, and D3 hybridomas had Russell bodies.

hybridomas constructed from +/+ mice (not shown). Also shown in Fig. 2 are five Mott cell hybridomas treated identically. Igs synthesized by the Mott cell hybridomas are indistinguishable from the μ chains synthesized by the normal hybridoma. Each cell line differs in the amount of IgM that is synthesized and released into the supernatant after 3 h. IgM is immunoprecipitated from the supernatants from the 1B9, A3, 2F3, and D3 Mott cell hybridomas, while IgM is undetectable in the supernatant from the D8 cell line. IgM precipitated from the SDS lysates of each of the five Mott cell hybridomas had a relative molecular weight similar to the μ chains solubilized by NP-40. Also, our anti-μ is H chain specific (not shown) and the data in Fig. 2 show that L chains are associated with the μ chains from Russell bodies. The fainter band visible in most immunoprecipitates is probably J chain.

The relative molecular mass of the κ chains from the Mott cell hybridomas were heterogeneous, but similar heterogeneity was observed in a panel of hybridomas made from hyperimmunized +/+ mice (not shown). Therefore, although we cannot rule out a role for aberrant κ chains in these hybridomas, we can say that similar heterogeneity is seen in normal hybridomas.

Pulse-chase Experiments

To quantify the secretory defect in Mott cell hybridomas, the $t_{1/2}$ of intracellular Ig was estimated by pulse-chase experiments. To eliminate the contribution from secreted IgM, we used the Mott cell hybridoma that secreted undetectable amounts of IgM. To solubilize the total intracellular pool of Ig, cells were treated with 1% SDS before immunoprecipitation. In Fig. 3, a normal IgM-secretor, "2E7", and the Mott cell hybridoma, "D8", were pulsed with ^{35}S-methionine for 15 min and the newly synthesized proteins were chased in medium without radioactive methionine for up to 12 h. IgM was immunoprecipitated and subjected to SDS-PAGE and fluorography. The rate of disappearance of Ig was much slower from hybridomas with Russell bodies. The $t_{1/2}$ of intracellular μ chains (78,000 M_r) was estimated by densitometric scans of each lane. Normal intracellular μ chains dis-

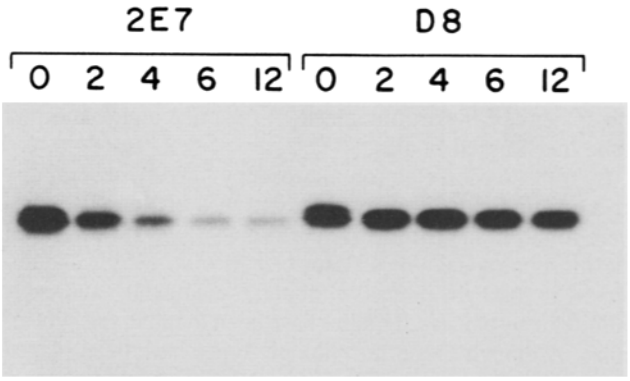

Figure 3. Extended half life of intracellular Ig in Mott cell hybridomas. Total intracellular Ig was solubilized from a normal hybridoma, 2E7, and a hybridoma with Russell bodies, D8. Hybridomas had been pulsed with ^{35}S-methionine and labeled proteins were chased for 0, 2, 4, 6, and 12 h. Total intracellular Ig was solubilized in 1% SDS. IgM was immunoprecipitated from each lysate and subjected to SDS-PAGE and fluorography. One the μ chain region of the fluoroautograph is shown.

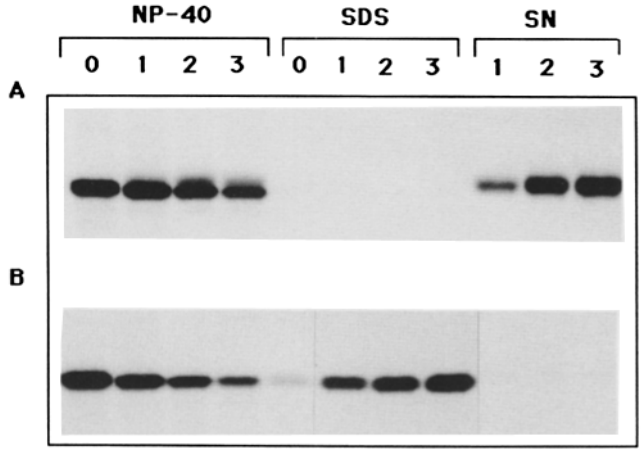

Figure 4. Deposition of Ig in Russell bodies occurs rapidly. Hybridomas were pulsed with ^{35}S-methionine and chased for 0, 1, 2, and 3 h. Ig was immunoprecipitated from the intracellular, NP-40–soluble material (*NP-40*), from the Russell bodies (*SDS*), and from the supernatants (*SN*), (*A*) Normal hybridoma (2E7). (*B*) Mott cell hybridoma (D8). Immunoprecipitates were subjected to SDS-PAGE and fluorography. Only the μ chain region of the fluoroautograph is shown.

appear with a $t_{1/2}$ of 2–3 h. The $t_{1/2}$ of intracellular μ chains from Mott cell hybridomas was estimated to be 24–30 h.

We examined the kinetics of the deposition of Ig into Russell bodies by a similar pulse–chase experiment in which the insoluble intracellular IgM was discriminated from soluble intracellular IgM. Mott cell hybridomas and normal hybridomas were pulsed with ^{35}S-methionine, as described above, and chased for 0, 1, 2, and 3 h. The hybridomas were first homogenized in 0.5% NP-40, in which the Russell bodies were insoluble. The Russell bodies were solubilized by homogenizing the insoluble material from the NP-40 lysate in 1% SDS (heretofore referred to as the SDS lysate). IgM was immunoprecipitated from the supernatants, the NP-40 lysates, and the SDS lysates. IgM from the normal hybridoma (2E7) appears in the supernatant (Fig. 4 *A*, *SN*) simultaneous with its disappearance from the intracellular pool (Fig. 4 *A*, NP-40). In contrast, IgM from the Mott cell hybridoma (D8) appeared in the SDS lysate (Fig. 4 *B*, *SDS*) as it disappeared from the NP-40 lysates (Fig. 4 *B*, NP-40). No detectable Ig appears in the supernatant from the Mott cell hybridoma (Fig. 4 *B*, *SN*). Also, the normal hybridoma accumulated no IgM in the SDS lysate (Fig. 4 *A*, *SDS*), which is consistent with the absence of Russell bodies. Densitometric scans of the fluoroautograph confirmed that the disappearance of μ chains from the NP-40 lysate was accelerated in the Mott cell hybridoma compared to the normal IgM secretor. In addition, the μ chains in the NP-40 lysates from the normal hybridoma could be discriminated into a lower relative molecular weight species and a larger relative molecular weight species that appeared with time. Most likely, this increase in relative molecular weight was caused by processing of the carbohydrate side chains of the μ chains (15). Only the more immature form was observed in the NP-40 lysates from the Mott cell hybridoma. These observations are consistent with a rapid deposition of IgM into Russell bodies in the RER.

Characterization of the Secretory Defect at the Cellular Level

Initially, the myeloma cell line used as the fusion partner was the Ig nonproducer, SP2/0; however, to examine the effect of the secretory defect on normal Ig synthesis and secretion, we fused cervical lymph node cells from *me^v/me^v* mice to the IgG1-secretor, P3X63Ag-8, from which SP2/0 was derived. A similar frequency of hybridomas with Russell bodies was obtained with the P3X63Ag-8 parent (27/85) as when SP2/0 was used in a parallel fusion (11/35). Mott cell hybridomas derived from the P3X63Ag-8 cell line synthesize both the MOPC 21 paraprotein (IgG1) and IgM from the *me^v/me^v* lymph node cells. Shown in Fig. 5 are Igs from the double producer that were immunoprecipitated from the 0.5% NP-40 lysates and the SDS lysates. Each lysate was divided into three parts and treated with normal rabbit serum, rabbit anti–mouse μ chain, or a polyspecific rabbit anti–mouse Ig, followed by protein A–bearing SACI. MOPC21 has a low affinity for protein A and consequently γ1 chains (50,000 M_r) were precipitated using normal rabbit serum, anti-μ chain, and the polyspecific antiserum. Although both IgM and IgG1 were precipitated from the NP-40 lysate (lanes 1–3), only IgM was precipitated from the SDS lysate, which is presumably derived from the Russell bodies (lanes *4–6*).

As an additional confirmation of these data, Mott cell hybridomas that synthesized both IgM and IgG1 were prepared for TEM and processed for protein A immunogold staining. Thin sections were treated with normal rabbit serum, rabbit anti–mouse γ1, or rabbit anti–mouse μ. Russell bodies from

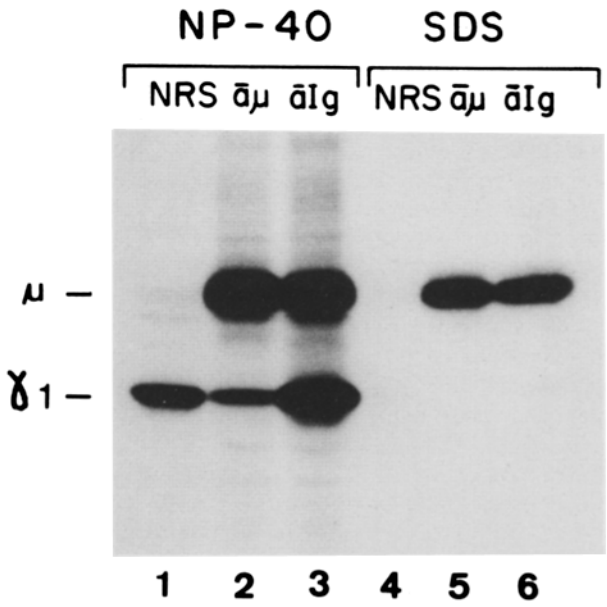

Figure 5. In IgM and IgG1-producing cell lines, only IgM was found in the Russell bodies. Hybridomas that synthesized *me^v/me^v*-derived IgM and normal IgG were labeled with ^{35}S-methionine. Igs were precipitated from the NP-40 lysate (lanes 1–3) and the insoluble material from this lysate, solubilized in SDS (lanes *4–6*). Igs were treated with normal rabbit serum (*NRS*), rabbit anti–mouse μ, or a polyspecific rabbit anti–mouse Ig antiserum. Immune complexes were precipitated with protein A–bearing SACI organisms. Each precipitate was subjected to SDS-PAGE and fluorography. Only the heavy chain region of the fluoroautograph is shown.

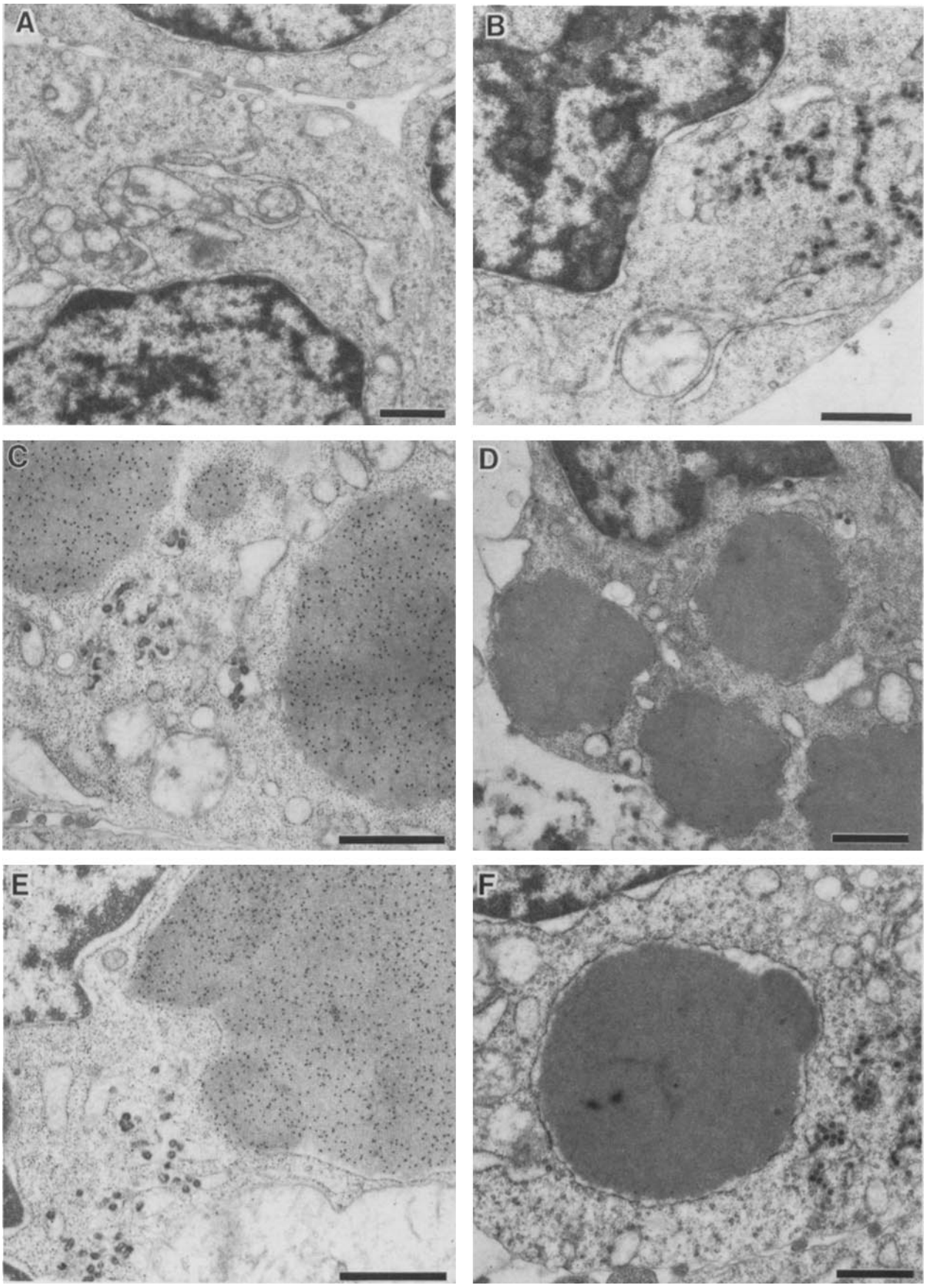
A
B
C
D
E
F

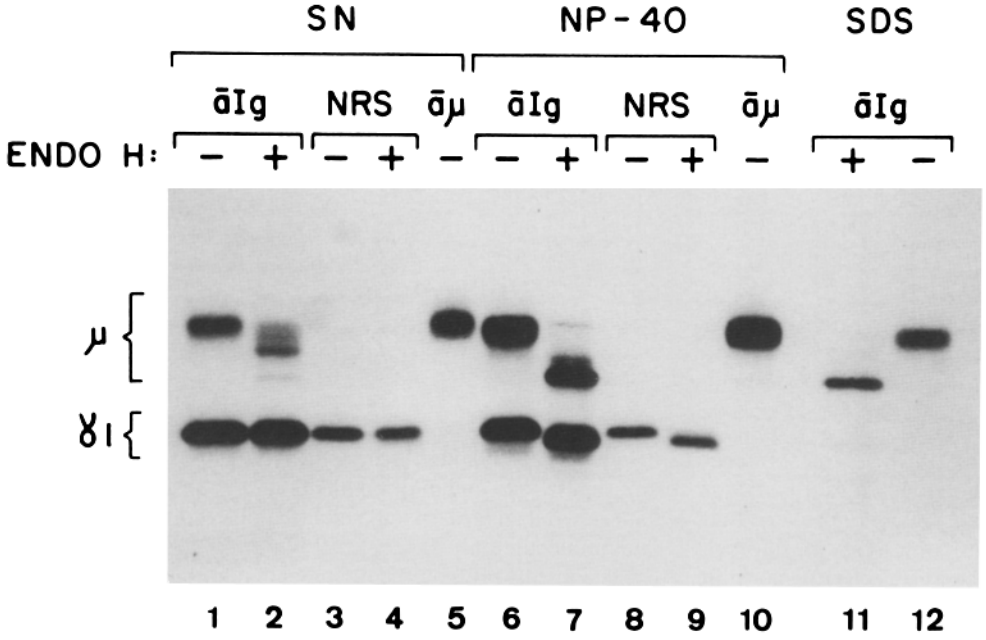

Figure 7. IgM in the supernatant of Mott cell hybridomas is bona fide secreted IgM. Nascent proteins from the double-producing hybridoma were labeled with ^{35}S-methionine for 3 h. Igs from the supernatant (lanes 1–5) and NP-40 lysate (lanes 6–10) were treated with normal rabbit serum (*NRS*), rabbit anti-mouse μ (*aμ*), or a polyspecific rabbit anti-mouse Ig antiserum (*aIg*). The SDS lysate (lanes *11* and *12*) was treated with aIg. Immune complexes were precipitated with protein A–bearing SACI organisms. Half of each precipitate was digested with endo H (+). Each sample was subjected to SDS-PAGE and fluorography. Only the heavy chain region of the fluoroautograph is shown.

IgM-producing Mott cell hybridomas stain intensely with rabbit anti-mouse μ followed by protein A-gold (Fig. 6, *C* and *E*). Rabbit anti-γ1 did not stain the Russell bodies in the hybridomas that synthesize both IgM and IgG1. Although the cells in Figures 6, *B* and *F* synthesize IgG1, the concentration in RER and Golgi complex is not sufficient to be detected by protein A-gold immunoelectron microscopy. Likewise, IgM in the RER and Golgi was undetectable. These data showed that while IgM was localized to the Russell bodies, consistent with the data in Fig. 5, IgG1 could not be detected in Russell bodies.

Mott Cell Hybridomas often Secrete Igs

Commonly, Ig was detected in the supernatants of Mott cell hybridomas. We sought to determine whether this Ig was derived from ruptured cells that released intracellular Ig or the Ig was bona fide secreted Ig. We took advantage of the observation that the high mannose forms of *N*-linked carbohydrates are sensitive to endo H digestion. High mannose carbohydrates are the predominant form of *N*-linked sugars found in the RER. Processing to the complex carbohydrate structures of mature glycoproteins in the golgi apparatus renders the carbohydrate side chains resistant to endo H digestion. For this analysis, we used the double producing cell line described above. In the fluoroautograph shown in Fig. 7, Igs precipitated from the supernatant, NP-40 lysate, and SDS lysate were subjected to endo H digestion and compared to undigested samples. The μ chain in the SDS lysate (lane *12*) was completely sensitive to endo H (lane *11*). This indicated that μ chains got high mannose *N*-linked sugars added, but further processing did not occur. This is consistent with the localization of the insoluble IgM to the RER. The NP-40 lysate contained both IgG1 and IgM; the γ1 chain, which only contains one *N*-linked sugar, was sensitive to endo H (compare lanes *8* and *9*). Similarly, intracellular μ from the NP-40 lysate was sensitive to endo H (lane *7*). Both IgM and IgG1 also were immunoprecipitated from the supernatant. Although γ1 chains were endo H resistant (compare lanes *3* and *4*), μ chains were not entirely resistant to endo H (lane *2*). This result was not unexpected because at least one of the five *N*-linked sugars on IgM can remain in the high mannose form after secretion (3). We have also observed that normal secreted μ chains remained partially sensitive to endo H (not shown). However, comparison of lanes *2*, *7*, and *11* indicated that IgM appearing in the supernatant had a different pattern of reaction products and was at least partially endo H resistant. Thus at least some of the *N*-linked carbohydrate chains on the secreted IgM molecules were processed to the complex form and appeared to be bona fide secreted IgM.

Cell rupture could also be ruled out by examination of the γ1 chains in Fig. 7. As seen in lanes *8* and *9*, the majority of intracellular γ1 was endo H sensitive. If Ig in the supernatant appeared after cell rupture, a portion of the γ1 in the supernatant should be endo H sensitive. However, the majority of γ1 immunoprecipitated from the supernatant was endo H resistant. These data confirm that Ig was secreted from these mutant cell lines, and significant amounts of Ig were not released by cell rupture.

Figure 6. Immunogold EM confirms that only IgM is condensed in Russell bodies. Hybridomas treated for immunogold EM. (*A* and *B*) The P3X63Ag8 cell line that contained no Russell bodies and secretes IgG1. (*C* and *D*) A Mott cell hybridoma derived from the SP2/0 fusion parent cell line that synthesized only IgM. (*E* and *F*) A Mott cell hybridoma derived from the P3X63Ag8 fusion parent cell line that synthesized both IgG1 and IgM. *A*, *C*, and *E* were stained with rabbit anti-μ followed by gold-labeled protein A. *B*, *D*, and *F* were stained with rabbit anti-γ1 followed by gold labeled protein A. No gold deposition occurred in similar sections when normal rabbit serum replaced the rabbit antisera (not shown). Bars, μ.

Discussion

We have analyzed the defects associated with abnormal plasmacytoid Mott cells that appear in lymphoid tissues of spontaneously autoimmune, *me^v/me^v* mice by creating a panel of hybridomas that contain Russell bodies. The hybridomas described in this report closely resemble Mott cells in vivo because of the high frequency of Mott cell hybridomas generated from *me^v/me^v* lymphoid tissues and the isotypes of Ig that are produced. Alanen et al. (1) described several Mott cell hybridomas obtained from autoimmune, NZB mice (1, 2), which, like *me^v/me^v* mice, accumulate many Mott cells. Whereas one-third of hybridomas from *me^v/me^v* mice had Russell bodies, <2% of hybridomas from NZB mice were identified as Mott cells. The most common isotype found in Mott cells in vivo is IgM (1, 35). All hybridomas obtained from *me^v/me^v* synthesized IgM; previously described Mott cell hybridomas are IgG1 or IgG3 (1), or only produce light chains (36, 39). Thus, these hybridomas may be the best models for determining the molecular defect(s) responsible for the appearance of Mott cells and the deposition of Ig in Russell bodies.

The Russell bodies are likely to be deposits of IgM as inclusion bodies. The hybridomas described here were selected for the presence of Russell bodies, a morphologic characteristic. These Russell bodies were electron-dense deposits of glycoprotein in RER-bound vesicles, which contained IgM molecules detected by immunoelectron microscopy (Fig. 6). Also, the Russell bodies remained intact in 0.5% NP-40. The most remarkable biochemical feature of these cell lines was the presence of a large intracellular pool of insoluble Ig. This insoluble Ig required strong denaturing conditions to solubilize. The insoluble Ig contains exclusively high mannose *N*-linked carbohydrate (Fig. 7), a characteristic of glycoproteins found in the RER. Thus, the data are consistent with the intracellular insoluble Ig localized to the Russell bodies.

Biochemical characterization of the insoluble Ig demonstrated that all of the hybridomas examined synthesized μ chains that are normal in relative molecular weight as judged by SDS-PAGE, and synthesize both H and L chains. This is in contrast to many Ig secretion mutants previously described that have sizable deletions in their Ig genes (32, 37) or synthesize only H or L chains (27). Though immunoglobulin binding protein, BiP, has been shown to be involved in proper assembly of Ig, we feel it unlikely that faulty interactions with BiP are responsible for Russell body formation. Ig isolated from Russell bodies included both H and L chains, and in preliminary experiments, IgM from Russell bodies, and also secreted Ig, appeared to be assembled properly. Hendershot et al. (12) demonstrated that mutant Igs that are assembled improperly do not associate with BiP and are secreted. However, it is possible that BiP will be found associated with improperly folded Ig (see below). We plan to investigate further the role of BiP in Ig synthesis and secretion by Mott cell hybridomas.

Hybridomas synthesizing both IgM and IgG1 were used to determine whether the secretory defect causing IgM molecules to be localized to Russell bodies affected the normal secretion of IgG1. Results of immunoprecipitation experiments and immunoelectron microscopy (Figs. 5 and 6) confirm that only *me^v/me^v*-derived IgM was localized to Russell bodies and IgG1 molecules were unaffected by the presence of Russell bodies. Also, non-Ig proteins synthesized and secreted by Mott cell hybridomas were also unaffected by the presence of Russell bodies (P. A. Schweitzer, unpublished results). Thus, the secretory defect was limited to the IgM molecule.

It has been proposed that Russell bodies appear when the amount of IgM synthesized by Mott cells exceeds the capacity of the cellular machinery required for secretion. We feel this explanation is inadequate for two reasons. First, Mott cell hybridomas that synthesize both IgM and IgG1 only contain IgM in the Russell bodies. Second, this hypothesis cannot account for cell lines that secreted no detectable Ig (e.g., *D8* in Fig. 2).

We interpret the data presented here to indicate that the secretory defects are intrinsic to the IgM molecule itself. However, even though many normal IgM-secreting cells are present in vivo and in our collection of hybridomas, we cannot rule out an IgM-specific, cellular defect that insolubilizes this molecule only.

The results presented here indicate that Russell bodies are similar to inclusion bodies that form when mutant proteins are improperly folded or assembled (26). Phenotypically, these Ig secretion mutants are remarkably similar to secretory defects found in patients with α_1-antitrypsin deficiency. Individuals homozygous for the Pi^Z allele of α_1-antitrypsin have decreased levels of serum α_1-antitrypsin and α_1-antitrypsin accumulates in RER-bound vesicles (6). A single amino acid substitution of lysine for glutamic acid is sufficient to cause the defect (16). This substitution disrupts an intramolecular salt bridge (23) that may be important for proper folding. However, Pi^Z alleles from different individuals have additional mutations (40), and considerable molecular heterogeneity in the α_1-antitrypsin proteins from different Pi^Z/Pi^Z individuals has been reported (13, 25). Thus it is not unlikely that the α_1-antitrypsin genes from different individuals have additional or different mutations that cause similar disruptions in tertiary structure of the protein and deposition of α_1-antitrypsin in inclusion bodies.

Similar phenotypes are also seen in secretion mutants of VSV-infected cells. Transport to the cell surface of the G protein of variants of VSV display heterogeneity in their sensitivity to temperature and tunicamycin (11, 20). The G protein aggregates intracellularly and displays decreased solubility in nonionic detergents under conditions where virion maturation is inhibited. These defects often affect tertiary or quaternary structure of the protein and can be traced to mutations in the G protein gene itself (8, 10, 18).

Thus, arguing by analogy to other known mutations, and from the data presented in this report, we conclude that Russell bodies are inclusion bodies, and the defect may be caused by abnormal or incomplete folding of the Ig molecule, leading to insolubility in the RER.

Because there are many normal plasma cells in *me^v/me^v* lymphoid tissues and many of the hybridomas from these experiments were phenotypically normal, it is likely that the defect is somatically derived. It is possible that a unique combination of Ig gene segments (V, D, J or combinations of V_L and V_H) produces these abnormal Igs. However, assuming there is no selective advantage for having secretory defects, the high frequency at which these hybridomas are obtained (30%) argues against this possibility.

An intriguing hypothesis for the formation of Russell

body-containing cells is that the Ig genes in Mott cells have accumulated deleterious somatic mutations during the process of somatic hypermutation, where the somatic mutation rate in Ig genes can be as high as 10^{-3} per base pair per cell division (21, 30). Under normal circumstances, clonal selection acts on cells which have fortuitously acquired Igs with increased affinity for antigen. However, cells with deleterious mutations in Ig genes would be unable to properly display the antigen receptor on the cell membrane and thus fail to be selected by antigen and disappear from the responding population. Indeed, it has been estimated that ≥25% of these mutations destroy the integrity of the V regions and these antibodies are lost from the repertoire (7).

We hypothesize that in tissues of *me^v/me^v* mice, B cells are spontaneously activated to proliferate and become plasma cells independent of the specificity (or presence) of surface Ig. In addition to autoantibodies commonly produced by these mutant mice, deleterious mutations accumulate that interfere with proper assembly, processing, or solubility of the Ig molecule. Therefore, clonal selection is circumvented, and these abnormal plasma cells appear. This hypothesis is consistent with the observation that Mott cells often appear in normal animals after mitogenic stimulation with crude bacterial preparations (38) or hyperactivation of the immune system by pathogens (28). Similarly, we have observed that Mott cells can be generated in vitro by mitogenic stimulation of normal spleen cells (P. A. Schweitzer, unpublished results). Further studies are needed to examine the validity of this hypothesis.

The authors thank Elaine Hall for expert technical assistance and Drs. Robert Evans and Edward Leiter for critical review of the manuscript.

This investigation was supported by grants CA20408 and DK07449 from the National Institutes of Health and grant IN155 from The American Cancer Society.

Received for publication 7 March 1991 and in revised form 15 March 1991.

References

1. Alanen, A., U. Pira, O. Lassila, J. Roth, and R. M. Franklin. 1985. Mott cells are plasma cells defective in immunoglobulin secretion. *Eur. J. Immunol.* 15:235–242.
2. Alanen, A., U. Pira, A. Colman, and R. M. Franklin. 1987. Mott cells: a model to study immunoglobulin secretion. *Eur. J. Immunol.* 17:1573–1577.
3. Anderson, D. R., P. H. Atkinson, and W. J. Grimes. 1985. Major carbohydrate structures at five glycosylation sites on murine IgM determined by high resolution ^{1}H-NMR spectroscopy. *Arch. Biochem. Biophys.* 243: 605–618.
4. Armstrong, J. A., R. L. Dawkins, and R. Horne. 1985. Retroviral infection of accessory cells and the immunological paradox in AIDS. *Immunol. Today.* 6:121–122.
5. Deleted in proof.
6. Carrell, R. W., J. Jeppsson, C. Laurell, S. O. Brennan, M. C. Owen, L. Vaughn, and D. R. Boswell. 1982. Structure and variation of human α_1-antitrypsin. *Nature (Lond.).* 298:329–334.
7. Cumano, A., and K. Rajewsky. 1986. Clonal recruitment and somatic mutation in the generation of immunological memory to the hapten NP. *EMBO (Eur. Mol. Biol. Organ.) J.* 5:2459–2468.
8. Doms, R. W., A. Ruusala, C. Machamer, J. Helenius, A. Helenius, and J. K. Rose. 1988. Differential effects of mutations in three domains on folding, quaternary structure, and intracellular transport of vesicular stomatitis virus G protein. *J. Cell Biol.* 107:89–99.
9. Gefter, M. L., D. H. Margulies, and M. D. Scharff. 1977. A simple method for polyethylene glycol-promoted hybridization of mouse myeloma cells. *Somatic Cell Genetics.* 3:231–236.
10. Gething, M., K. McCammon, and J. Sambrook. 1986. Expression of wild-type and mutant forms of influenza hemagglutinin: the role of folding in intracellular transport. *Cell.* 46:939–950.
11. Gibson, R., S. Schlesinger, and S. Kornfeld. 1979. The nonglycosylated glycoprotein of vesicular stomatitus virus is temperature-sensitive and undergoes intracellular aggregation at elevated temperatures. *J. Biol. Chem.* 254:3600–3607.
12. Hendershot, L., D. Bole, G. Kohler, and J. F. Kearney. 1987. Assembly and secretion of heavy chains that do not associate posttranslationally with immunoglobulin heavy chain-binding protein. *J. Cell Biol.* 104: 761–767.
13. Hercz, A., and M. Barton. 1977. The purification and properties of human α_1-antitrypsin (α_1-antiprotease), variant Z. *Eur. J. Biochem.* 74:603–610.
14. Hotchkiss, R. D. 1948. A microchemical reaction resulting in the staining of polysaccharide structures in fixed tissue preparations. *Arch. Biochem.* 16:131–141.
15. Kehry, M., S. Ewald, R. Douglas, C. Sibley, W. Raschke, D. Fambrough, and L. Hood. 1980. The immunoglobulin μ chains of membrane-bound and secreted IgM molecules differ in their C-terminal segments. *Cell.* 21:393–406.
16. Kidd, V. J., R. B. Wallace, K. Itakura, and S. L. C. Woo. 1983. α_1-antitrypsin deficiency detection by direct analysis of the mutation in the gene. *Nature (Lond.).* 304:230–234.
17. Kohler, G., and C. Milstein. 1975. Continuous cultures of fused cells secreting antibody of predefined specificity. *Nature (Lond.).* 256:495–497.
18. Kreis, T. E., and H. F. Lodish. 1986. Oligomerization is essential for transport of vesicular stomatitis viral glycoprotein to the cell surface. *Cell.* 46:929–937.
19. Laemmli, U. K. 1970. Cleavage of structural proteins during the assembly of the head of bacteriophage T4. *Nature (Lond.).* 227:680–689.
20. Leavitt, R., S. Schlesinger, and S. Kornfeld. 1977. Impaired intracellular migration and altered solubility of nonglycosylated glycoproteins of vesicular stomatitus virus and Sindbis virus. *J. Biol. Chem.* 252:9018–9023.
21. Levy, N. S., U. V. Malipiero, S. G. Lebecque, and P. J. Gearhart. 1989. Early onset of somatic mutation in immunoglobulin V_H genes during the primary immune response. *J. Exp. Med.* 169:2007–2019.
22. Lisco, H. 1942. Russell bodies occurring in the lymph follicles of the intestinal tract of pigs. *Anat. Rec.* 82:59–66.
23. Loebermann, H., R. Tokuoka, J. Deisenhofer, and R. Huber. 1984. Human α_1-proteinase inhibitor: crystal structure analysis of two crystal modifications, molecular model and preliminary analysis of the implications for function. *J. Mol. Biol.* 177:531–557.
24. Maldonado, J. E., A. L. Brown, E. D. Bayrd, and G. L. Pease. 1966. Cytoplasmic and intranuclear electron-dense bodies in the myeloma cell. *Arch. Pathol.* 81:484–500.
25. Miller, R., M. S. Kuhlenschmidt, C. J. Coffee, I. Kuo, and R. H. Glew. 1976. Comparison of the chemical, physical, and survival properties of normal and Z-variant α_1-antitrypsins. *J. Biol. Chem.* 251:4751–4757.
26. Mitraki, A., and J. King. 1989. Protein folding intermediates and inclusion body formation. *Biotechnology.* 7:690–697.
27. Morrison, S. L., and M. D. Scharff. 1975. Heavy chain-producing variants of a mouse myeloma cell line. *J. Immunol.* 114:655–659.
28. Mott, F. W. 1905. Observations on the brains of men and animals infected with various forms of trypanosomes. *Proc. Royal Soc.* 76:235–242.
28*a*. Roth, J., M. Bendayan, and L. Orci. 1978. Ultrastructural localization of intracellular antigens by the use of Protein A-gold complex. *J. Histochem. Cytochem.* 26:1074–1081.
29. Russell, W. 1809. An address on a characteristic organism of cancer. *Brit. Med. J.* 2:1356–1260.
30. Sablitzky, F., G. Wildner, and K. Rajewsky. 1985. Somatic mutation and clonal expansion of B cells in an antigen-driven immune response. *EMBO (Eur. Mol. Biol. Organ.) J.* 4:345–350.
31. Shulman, M., C. D. Wilde, and G. Kohler. 1978. A better cell line for making hybridomas secreting specific antibodies. *Nature (Lond.).* 276:269–270.
32. Shulman, M. J., S. Heusser, C. Filkin, and G. Kohler. 1982. Mutations affecting the structure and function of immunoglobulin M. *Mol. Cell Biol.* 2:1033–1043.
33. Shultz, L. D., and C. L. Sidman. 1987. Genetically determined murine models of immunodeficiency. *Annu. Rev. Immunol.* 5:367–403.
34. Shultz, L. D., D. R. Coman, C. L. Bailey, W. G. Beamer, and C. L. Sidman. 1984. "Viable motheaten," a new allele at the motheaten locus. I. Pathology. *Amer. J. Pathol.* 116:179–192.
35. Shultz, L. D., D. R. Coman, B. L. Lyons, C. L. Sidman, and S. E. Taylor. 1987. Development of plasmacytoid cells with Russell bodies in autoimmune "viable motheaten" mice. *Amer. J. Pathol.* 127:38–50.
36. Weiss, S., P. D. Burrows, J. Meyer, and M. R. Wabl. 1984. A Mott cell hybridoma. *Eur. J. Immunol.* 14:744–748.
37. Weitzman, S., and M. D. Scharff. 1975. Mouse myeloma mutants blocked in the assembly, glycosylation and secretion of immunoglobulin. *J. Mol. Biol.* 102:237–252.
38. White, R. G. 1954. Observations on the formation and nature of Russell bodies. *Brit. J. Exp. Pathol.* 35:365–376.
39. Winberry, L., A. Marks, and R. Baumal. 1980. Immunoglobulin production and secretion by variant clones of the MOPC 315 mouse myeloma cell line. *J. Immunol.* 124:1174–1182.
40. Yoshida, A., J. Lieberman, L. Gaidulis, and C. Ewing. 1976. Molecular abnormality of human α_1-antitrypsin variant (Pi-ZZ) associated with plasma activity deficiency. *Proc. Natl. Acad. Sci. USA.* 73:1324–1328.